Electronic Supplementary Material (ESI) for Chemical Communications.

Inducing High Activity of a Thermophilic Enzyme at Ambient Temperatures by Directed Evolution

Guangyue Li, Miguel A. Maria-Solano, Adrian Romero-Rivera, Sílvia Osuna and Manfred T. Reetz**

Materials and chemicals 3
Methods 3
Docking acetophenone (**1a**) into WT TbSADH 3
PCR based methods for library construction of TbSADH 3
Primer design and library creation of TbSADH 4
Screening procedures 4
Protein expression and purification 4
Activity assay 5
Determination of kinetic parameters 5
Determination of thermostability by circular dichroism (CD) 5
Acetophenone (**1a**) reduction catalyzed by WT TbSADH, and variants TbSADH-1 and TbSADH-2 at 30°C, 45°C and 60°C. 5
Acetophenone (**1a**) reduction catalyzed by variants TbSADH-1 and TbSADH-2 at 200mM, 500mM, 1M and 2M concentration. 6
Substrate **1b** reduction catalyzed by WT TbSADH, and variants TbSADH-1 and TbSADH-2. 6
Substrate **1c-d** reduction catalyzed by WT TbSADH, variants ADH-1 and ADH-2. 6
Molecular dynamics (MD) simulations. 6
Supplementary movies of the MD simulations 7
Schemes, Tables and Figures 7
Scheme S1. Prelog and anti-Prelog selectivity for model ketone reductions catalyzed by TbSADH. 7
Table S1. Screening results of single site saturation mutagenesis at positions C37, S39, I49, A85, I86, L107, W110, T154, Y267, C283, M285, L294 and C295 towards acetophenone (1a). 7
Table S2. The code used for the construction of library A. 8
Table S3. Screening results of library A towards acetophenone (**1a**) 8
Table S4. Reduction of acetophenone (**1a**) (50mM) using purified WT TbSADH and best variants at different temperatures. 9
Table S5. Reduction of acetophenone (**1a**) at different concentrations using whole cells of WT TbSADH and best variants at 30°C. 9
Table S6. Kinetics of WT TbSADH, and variants TbSADH-1 and TbSADH-2 towards substrate **1b-d** 10
Table S7. Reduction of compound **1b** (50mM) using purified WT TbSADH and best variants at 30°C. 10
Table S8. The reduction of compound **1c-d** (10mM) using whole cells of wt TbSADH and best variants at 30°C. 11
Table S9. Measured melting temperature (T_m) of WT TbSADH, variants TbSADH-1 and

TbSADH-2 using circular dichroism (CD) 11
Table S10. List of primers for TbSADH libraries. 11
Table S11. Conditions for GC analyses. 12
Table S12. Volume calculated (in Å^3) for WT and A85G/I86A variant in the *apo* state along 100 frames from the MD simulations where the co-factor is not displaced from the enzyme active site. Calculations were done using POVME 2.0.[20] 13
Figure S1. Structural resistance of WT TbSADH(green), TbSADH-1(red) and TbSADH-2(blue) to elevated temperatures was determined as thermal denaturation in phosphate buffer (50 mM, pH 7.4). F_d refers to the unfolded fraction. 14
Figure S2. Construction of library A covering positions 85, 86, 110, 283, 285 and 294 using overlap PCR method. 14
Figure S3. GC profiles of **1a** to **2a** 15
Figure S4. GC profiles of **1b** to **2b** 16
Figure S5. GC profiles of **1c** to **2c** 17
Figure S6. GC profiles of **1d** to **2d** 18
Figure S7. Overlay of some representative MD snapshots for WT (A 30°C, C 45°C) and A85G/I86A variant (B 30°C, D 45°C) in the *apo* state. Average values of Root Mean Square Fluctuation (RMSF) of all residues computed from the MD simulations (where the cofactor is not displaced from the active site) in the *apo* state (C). 19
Figure S8. Representation of the Ramachandran plots of residues M106 (A, B), and L107 (C, D) for WT (green) and A85G/I86A variant (red) for all MD simulations in the *apo* state at 30°C. 20
Figure S9. Active site volume representation of the most populated cluster from the MD simulations in the *apo* state for WT (A), and A85G/I86A variant (B) 21
Figure S10. Representations of the most important non-covalent interactions (in green) between the substrate 1a and the active site for WT (A) and A85G/I86A variant (B) 21
Figure S11. Overlay of some representative MD snapshots for WT with 1a in *pro*-(S) conformation (A 30°C, C 45°C) and A85G/I86A variant with 1a in *pro*-(R) conformation (B 30°C , D 45°C). 22
References 23

Materials and chemicals

KOD Hot Start DNA Polymerase was obtained from Novagen. Restriction enzyme *Dpn* I was bought from NEB. The oligonucleotides were synthesized by Life Technologies. Plasmid preparation kit was ordered from Zymo Research, and PCR purification kit was bought from QIAGEN. DNA sequencing was conducted by GATC Biotech. All commercial chemicals were purchased from Sigma-Aldrich, Tokyo Chemical Industry (TCI) or Alfa Aesar.

Methods

Docking acetophenone (1a) into WT TbSADH

The X-ray structure[1] of TbSADH was used as the basis for docking calculations. The models of WT TbSADH was prepared as in a previous study.[2] Substrate acetophenone (**1a**) was prepared for docking using ChemDraw. Docking to the WT TbSADH was performed using autodock vina. Ten docking poses were requested and a constraint was applied such that only the docking poses in which the substrate coordinates to the active site zinc ion were saved.

PCR based methods for library construction of TbSADH

Libraries were constructed using Over-lap PCR and megaprimer approach with KOD Hot Start polymerase. 50 μL reaction mixtures typically contained 30 μL water, 5 μL KOD hot start polymerase buffer (10×), 3 μL 25 mM $MgSO_4$, 5 μL 2 mM dNTPs, 2.5 μL DMSO, 0.5 μL (50~100 ng) template DNA, 100 μM primers Mix (0.5 μL each) and 0.5 μL KOD hot start polymerase. The PCR conditions for short fragment: 95 °C 3 min, (95 °C 30 sec, 56 °C 30 sec, 68 °C 40 sec) × 30 cycles, 68 °C 120 sec. For mega-PCR: 95 °C 3 min, (95 °C 30 sec, 60 °C 30 sec, 68 °C 5 min 30 sec) × 28 cycles, 68 °C 10 min. The PCR products were analyzed on agarose gel by electrophoresis and purified using a Qiagen PCR purification kit. 2 μL NEB CutSmart™ Buffer and 2 μL *Dpn* I were added in 50 μL PCR reaction mixture and the digestion was carried out at 37 °C for 7 h. After *Dpn* I digestion, the PCR products 1.5 μL were directly transformed into electro-competent *E. coli* BL21(DE3) to create the final library for Quick Quality Control (QQC)[3] and screening.

Primer design and library creation of TbSADH

The previous constructed TbSADH single site saturation mutagenesis libraries at positions C37, S39, A85, W110, Y267, L294 and C295 in our lab were used for screening in this experiment. Other libraries were constructed as described below. Primer design and library construction depend upon the particular amino acid chosen, and in the case of TbSADH involves six single sites saturation mutagenesis and library A (covering sites 85, 86, 110, 283, 285 and 294 saturation mutagenesis): 1) Amplification of the short fragments of TbSADH using mixed primers I49NNK-F/49NNK-R, I86NNK-F/ I86NNK-R, L107NNK-F/ L107NNK-R, T154NNK-F/ T154NNK-R, C283NNK-F/C283NNK-R, M285NNK-F/M285NNK-R, 85+86-F/110-R, 110-F/283+285-R and 283+285-F/294-R for Library I49NNK, I86NNK, L107NNK, T154NNK, C283NNK, M285NNK and A, respectively; 2) Over-lap PCR using the PCR products of 85+86-F/110-R, 110-F/283+285-R and 283+285-F/294-R as template and mixed primers 85+86-F/294-R; 3) Amplification of the whole plasmid TbSADH using the PCR products of I49NNK-F/49NNK-R, I86NNK-F/ I86NNK-R, L107NNK-F/ L107NNK-R, T154NNK-F/ T154NNK-R, C283NNK-F/C283NNK-R, M285NNK-F/M285NNK-R and over-lap PCR product of step2 as megaprimers, leading to the final variety plasmids for library generation. All the primers used are listed in Table S10. The PCR products

were digested by *Dpn* I and transformed into electro-competent *E. coli*BL21 (DE3) to create the library for screening.

Screening procedures

Colonies were picked and transferred into deep-well plates containing 300 μL LB medium with 50 ug/mL kanamycin and cultured overnight at 37 °C with shaking. An aliquot of 120 μL was transferred to glycerol stock plate and stored at −80 °C. Then, 800 μL TB medium with 0.2 mM IPTG and 50 μg/mL kanamycin was added directly to the culture plate for 8 h at 30 °C with shaking for protein expression. The cell pellets were harvested, then washed with 400μL of 50 mM, pH 7.4 potassium phosphate buffer and centrifuged for 10 min 4000 rpm at 4 °C. The cell pellets were resuspended in 400 μL of the same buffer (adding 5mM DTT, 10μM $ZnCl_2$) with 6 U DNase I and 1 mg/mL lysozyme for breaking the cell at 30 °C for 1 h with shaking. The crude lysate was centrifuged for 30 min 4000 rpm at 4 °C. A quantity of 20 μL of supernatant was transferred into new microliter- plates, and the activity was detected using the activity assay shown in below. Then the relative activity was obtained after comparing with the activity of WT TbSADH.

Protein expression and purification

E. coli BL21 (DE3) cells carrying the recombinant plasmid were cultivated in 5 mL LB medium containing kanamycin (50 ug/mL) overnight at 37°C. The overnight culture was inoculated into 500 mL of TB medium containing kanamycin (50 ug/mL) and grown at 37°C. The culture was induced by addition of isopropyl β-D-1-thiogalactopyranoside (IPTG) with a final concentration of 0.2 mM when OD_{600} reached 0.6, and then allowed to grow for additional 12 h at 25°C. After centrifugation at 6000g for 15min at 4 °C, the bacterial pellet was washed with phosphate buffer (50 mM, pH 7.4), and resuspended in a phosphate buffer (20 mM, pH 7.4) containing 0.5 M of NaCl and 20 mM of imidazole. The cells were lysed by sonication and the supernatant was collected by centrifugation at 10000g for 60 min at 4 °C. Protein purification was performed using an AKTA Purifier 10 system with UNICORN 5 software (GE Healthcare). The WT and mutants were purified using affinity chromatography with a HisTrapTM FF crude column (GE, USA). The column was pre-equilibrated with 50 mL of equilibrium buffer (20 mM phosphate buffer, 0.5 M NaCl, 20 mM imidazole, pH 7.4). The sample (30 mL) was loaded with a flow rate of 2.0 mL/min. After washing with 50 mL of the equilibrium buffer, the bounded target protein was washed with 10−500 mM imidazole solution containing 500 mM NaCl and 20 mM potassium phosphate (pH 7.4). The target protein fraction was collected and desalted through a HiPrep 26/10 desalting column (GE Healthcare) against 20 mM phosphate buffer containing 5mM DTT, 10μM $ZnCl_2$ and 100 mM NaCl (pH 7.4). Protein concentration was measured using the Bradford method.

Activity assay

Enzyme activity was determined in a 0.2 mL volume of phosphate buffer (20 mM, pH 7.4) containing substrate (10 mM), NADPH (0.5 mM), 5mM DTT, 10μM $ZnCl_2$ and 20 uL enzyme. The substrate was dissolved in acetonitrile, which did not exceed 5% of the total volume. The reaction was initiated by the addition of the enzyme, and monitored for 1.2 min with SPECTRAMAX M5 (Molecular Devices, USA) at 30°C. The activity was determined by measuring NADPH oxidation from the decrease in absorbance at 340 nm using a molar absorption coefficient of 6.22 mM^{-1} cm^{-1}. One unit of enzyme activity was defined as the amount of enzyme catalyzing the conversion of 1

umol NADPH per minute.

Determination of kinetic parameters

The kinetic parameters were obtained by measuring the initial velocities of the enzymic reaction and curve-fitting according to the Michaelis−Menten equation. The activity assay was performed in a mixture containing 0.7 mM of NADPH and varying concentration of substrate **1a** (0.5−30 mM), **1b** (0.5−15 mM), **1c** (0.5−20 mM) and **1d** (0.5−10 mM). All experiments were conducted in triplicate.

Determination of thermostability by circular dichroism (CD)

CD spectra were recorded using Jasco J-810 spectropolarimeter (Jasco, Tokyo, Japan) equipped with the Peltier cell holder. Thermal unfolding of tested enzymes was followed by monitoring the ellipticity at 222 nm over the temperature range from 30 to 110°C with a resolution of 0.1°C and heating rate of 2°C min^{-1}. Recorded thermal denaturation curves were fitted to sigmoidal curves using Origin 6.1 software. The melting temperature (T_m), the temperature at which half of the enzyme is in an unfolded state, was evaluated as the midpoint of the normalized thermal transition.

Acetophenone (1a) reduction catalyzed by WT TbSADH, and variants TbSADH-1 and TbSADH-2 at 30°C, 45°C and 60°C.

A 1mL mixture of 50mM acetophenone (**1a**), 0.1mM $NADP^+$, 5mM DTT, 10μM $ZnCl_2$, 150uL 2-propanol (15%) and 0.8 mg purified WT TbSADH (TbSADH-1 or TbSADH-2) in PBS buffer solution (50mM, pH 7.4) was stirred at 30°C, 45°C and 60°C. Then 0.1mL reaction product were extracted with ethyl ether (1 mL) at 0.5, 1.5 and 20h, respectively.

Acetophenone (1a) reduction catalyzed by variants TbSADH-1 and TbSADH-2 at 200mM, 500mM, 1M and 2M concentration.

A 1mL mixture of 200mM (500mM, 1M or 2M) acetophenone (**1a**), 0.1mM $NADP^+$, 5mM DTT, 10μM $ZnCl_2$, 300uL 2-propanol (500uL 2-propanol for 500mM, 1M and 2M acetophenone) and recombinant expression whole cells of TbSADH-1 or TbSADH-2 (OD_{600}=50) in PBS buffer solution (50mM, pH 7.4) was stirred at 30°C. Then 0.1mL reaction product were extracted with ethyl ether (1 mL) at 4 and 20h, respectively. 400ul iso-propanol were added in the reaction system at 20h for pushing the reaction toward reduction. Then 0.1mL reaction product were extracted with ethyl ether (1 mL) at 36h.

Substrate 1b reduction catalyzed by WT TbSADH, and variants TbSADH-1 and TbSADH-2.

A 1mL mixture of 50mM **1b**, 0.1mM $NADP^+$, 5mM DTT, 10μM $ZnCl_2$, 150uL 2-propanol (15%) and 0.2 mg purified WT TbSADH (TbSADH-1 or TbSADH-2) in PBS buffer solution (50mM, pH 7.4) was stirred at 30°C. Then 0.1mL reaction product were extracted with ethyl ether (1 mL) at 1, 3 and 20h, respectively.

Substrate 1c-d reduction catalyzed by WT TbSADH, variants ADH-1 and ADH-2.

A mixture of 10 mM substrate **1c-d**, 0.1mM $NADP^+$, 5mM DTT, 10μM $ZnCl_2$, 150uL 2-propanol and recombined expression whole cells of WT TbSADH, ADH-1 or ADH-2 (OD_{600}=30) in 1.0 mL PBS buffer solution (50mM, pH 7.4) was stirred at 30°C and then extracted with ethyl ether (1 mL)

at 20h.

Molecular dynamics (MD) simulations.

MD simulations in explicit water were performed using AMBER 16 package[4] and starting from the PDB structure: 1YKF.[1] The A85G/I86A variant was generated using the mutagenesis tool included in PyMOL (http://www.pymol.org). Parameters for substrate **1a** for the MD simulations were generated within the *antechamber* module of AMBER 16 using the general AMBER force field (GAFF),[5] with partial charges set to fit the electrostatic potential generated at the B3LYP/6-31G(d) level by the restrained electrostatic potential (RESP) model.[6] The charges were calculated according to the Merz-Singh-Kollman scheme[7, 8] using Gaussian 09.[9] Amino acid protonation states were predicted using the H++ server (http://biophysics.cs.vt.edu/H++).[10] We have used the bonded model for Zn metal center, the residues of the first coordination sphere and either the substrate or a water molecule (*apo* state) bound.[11] In particular we used the Seminario approach[12] to obtain the metal parameters needed for the simulation as implemented in Prof. Ryde program.[13] The optimization, frequencies and charge calculations to obtain the parameters was done at the B3LYP/6-31G(d) level using Gaussian 09.[7] The parameters for NAD(P)H were extracted from previous studies by Prof. Ryde.[14,15] The wild-type enzyme (PDB: 1YKF) and variant were solvated in a pre-equilibrated truncated cuboid box with a 10-Å buffer of TIP3P[16]water molecules using the AMBER16 *leap* module, resulting in the addition of *ca.* 9,000 solvent molecules. The system was neutralized by addition of explicit counterions (Na^+ and Cl^-). All calculations were done using a modification of the *ff*99SB force field (*ff*94SB).[17] A two-stage geometry optimization approach was performed. The first stage minimizes the positions of solvent molecules and ions imposing positional restraints on solute by a harmonic potential with a force constant of 500 kcal mol^{-1} $Å^{-2}$, and the second stage is an unrestrained minimization of all the atoms in the simulation cell. The systems are gently heated using six 50-ps steps, incrementing the temperature 50 K each step (0–300 K, 30ºC and 0-315 K, 45ºC) under constant volume and periodic boundary conditions. Water molecules were treated with the SHAKE algorithm such that the angle between the hydrogen atoms is kept fixed. Long-range electrostatic effects were modeled using the particle-mesh-Ewald method.[18] An 8-Å cutoff was applied to Lennard-Jones and electrostatic interactions. Harmonic restraints of 10 kcal/mol were applied to the solute, and the Langevin equilibration scheme was used to control and equalize the temperature. The time step was kept at 1 fs during the heating stages, allowing potential inhomogeneities to self-adjust. Each system was then equilibrated without restrains for 2 ns with a 2-fs timestep at a constant pressure of 1 atm and temperature of 300 K. After the systems were equilibrated in the NPT ensemble, 5 independent two hundred nanosecond MD simulations were performed under the NVT ensemble and periodic-boundary conditions at 30 and 45ºC in the substrate-bound and *apo* states. Therefore, an accumulated simulation time of 1 microsecond has been obtained for each variant (WT and A85G/I86A) at each temperature (30 and 45ºC) in both *apo* and substrate-bound states.

Supplementary movies of the MD simulations

Representative frames from two independent MD simulations for: the WT enzyme in the *apo* state at 30ºC (WT_30.mp4) and at 45ºC (WT_45.mp4); A85G/I86A variant in the *apo* state at 30ºC (mutant_30.mp4) and at 45ºC (mutant_45.mp4).

Active site volume changes along one representative MD simulation for: the WT enzyme in the *apo*

state at 30ºC (volume_WT_30.mp4) and at 45ºC (volume_WT_45.mp4); the A85G/I86A variant in the *apo* state at 30ºC (volume_mutant_30.mp4), and at 45ºC (volume_mutant_45.mp4).

Schemes, Tables and Figures

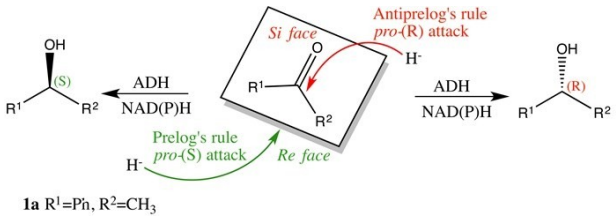

Scheme S1. Prelog and anti-Prelog selectivity for model ketone reductions catalyzed by TbSADH.

Table S1. Screening results of single site saturation mutagenesis at positions C37, S39, I49, A85, I86, L107, W110, T154, Y267, C283, M285, L294 and C295 towards acetophenone (**1a**).

Library	Positive hits	mutation	Relative activity
WT			100%
C37NNK	ND[a]		
S39NNK	ND		
I49NNK	ND		
A85NNK	LG-85-B10	A85G	1300%
I86NNK	LG-86-C6	I86C	1400%
	LG-86-F6	I86E	900%
	LG-86-H11	I86A	1500%
L107NNK	ND		
W110NNK	LG-110-B7	W110L	400%
	LG-110-G7	W110I	450%
	LG-110-F8	W110E	650%
T154NNK	ND		
Y267NNK	ND		
C283NNK	LG-283-E2	C283V	500%
M285NNK	LG-285-A10	M285V	400%
	LG-285-H6	M285L	300%
L294NNK	LG-294-H7	L294T	400%
	LG-294-F12	L294V	350%
C295NNK	ND		

a: no positive hits were detected.

Table S2. The code used for the construction of library A.

Entry	Positions	Code for mutation
1	A85	A and G
2	I86	I,C, E and A
3	W110	W,I, L and E
4	C283	C and V
5	M285	M, L and V
6	L294	L,T and V

Table S3. Screening results of library A towards acetophenone (**1a**).

Entry	Positive hits	mutation	Relative activity
1	WT		100%
2	LG137	A85G	1300%
3	LG228	A85G/I86A/C283V/M285L	1200%
4	LG234	I86C	1400%
5	LG349	I86A	1500%
6	LG587	A85G/I86C/C283V/M285L	1400%
7	LG685	A85G/C283V	1550%
8	LG853	A85G/I86A/L294V	1300%
9	LG1089 (**TbSADH-1**)	A85G/I86A	3200%
10	LG1532 (**TbSADH-2**)	A85G/I86C	3100%

Table S4. Reduction of acetophenone (**1a**) (50mM) using purified WT TbSADH and best variants at different temperatures.

Enzyme	time	Conversion rate (30°C)	Conversion rate (45°C)	Conversion rate (60°C)	ee (%)
WT TbSADH	0.5h	ND[a]	Trace[b]	Trace	
	1.5h	Trace	Trace	Trace	
	20h	4%	6%	8%	17% (*S*)
TbSADH-1	0.5h	80%	90%	93%	99% (*R*)
	1.5h	96%	97%	98%	99% (*R*)
TbSADH-2	0.5h	78%	86%	92%	99% (*R*)
	1.5h	96%	97%	97%	99% (*R*)

a: No peak is detected. b: The peak is too low to be calculated.

Table S5. Reduction of acetophenone (**1a**) at different concentrations using whole cells of WT TbSADH and best variants at 30°C.

Enzyme	**time**	**Conversion rate (200mM)**	**Conversion rate (500mM)**	**Conversion rate (1 M)**	**Conversion rate (2 M)**
TbSADH-1	4h	86%	72%	55%	37%
	20h[a]	86%	77%	66%	52%
	36h	93%	86%	76%	65%
TbSADH-2	4h	86%	72%	52%	38%
	20h[a]	86%	78%	66%	54%
	36h	93%	86%	76.5%	66%

a: 400ul iso-propanol were added in the reaction system at 20h.

Table S6. Kinetics of WT TbSADH, and variants TbSADH-1 and TbSADH-2 towards substrate **1b-d**.

1b	Enzyme	Mutations	Km (mM)	k_{cat} (min^{-1})	k_{cat}/Km (min^{-1} M^{-1})
30ºC	wt ADH		3.92±0.32	1.04±0.03	265
	ADH-1	A85G/I86A	4.70±0.23	177.79±2.84	37827
	ADH-2	A85G/I86C	11.12±1.89	187.06±15.01	16822
1c	Enzyme	Mutations	Km (mM)	k_{cat} (min^{-1})	k_{cat}/Km (min^{-1} M^{-1})
30ºC	wt ADH		1.65±0.08	2.98±0.03	1806
	ADH-1	A85G/I86A	14.62±2.55	18.94±1.74	1295
	ADH-2	A85G/I86C	12.46±2.15	13.59±1.16	1090
1d	Enzyme	Mutations	Km (mM)	k_{cat} (min^{-1})	k_{cat}/Km (min^{-1} M^{-1})
30ºC	wt ADH		1.07±0.06	2.38±0.04	2224
	ADH-1	A85G/I86A	4.23±0.63	8.23±0.94	1945
	ADH-2	A85G/I86C	5.30±0.65	4.75±0.58	896

Table S7. Reduction of compound **1b** (50mM) using purified WT TbSADH and best variants at 30°C.

Enzyme	**time**	**Conversion rate (30°C)**	**ee (%)**
WT TbSADH	1h	ND	
	3h	ND	
	20h	4%	26.6 % (*S*)
TbSADH-1	1h	96%	98% (*R*)
	3h	97%	98% (*R*)
TbSADH-2	1h	96%	98% (*R*)
	3h	97%	98% (*R*)

Table S8. The reduction of compound **1c-d** (10mM) using whole cells of wt TbSADH and best variants at 30°C.

substrate	enzyme	Conversion rate (%)	ee (%)	favored enantiomer
1c	wtTbSADH	99%	99%	*S*
	ADH-1	99%	99%	*S*
	ADH-2	99%	99%	*S*
1d	wtTbSADH	99%	99%	*S*
	ADH-1	99%	99%	*S*
	ADH-2	99%	99%	*S*

Table S9. Measured melting temperature (T_m) of WT TbSADH, variants TbSADH-1 and TbSADH-2 using circular dichroism (CD)

Entry	**Enzyme**	T_m
1	wt TbSADH	90°C
2	TbSADH-1	84°C
3	TbSADH-2	87.5°C

Table S10. List of primers for TbSADH libraries.

Library	Primers		Sequence (5' to 3')
I49NNK	I49NNK-F		TTTGAAGGCGCC**NNK**GGCGAAAGACATAACA
	I49NNK-R		GTGATATCCTCTTTGTACTTCAG
I86NNK	I86NNK-F		CACTTCGGACATTCATACCGTTT
	I86NNK-R		CCAATCAGGGGT**MNN**AGCTGGCACAACAA
L107NNK	L107NNK-F		ATTTTAAACCTGGTGATCGCGT
	L107NNK-R		AATTTCCAGCCTGC**MNN**CATTCCACCGGAG
T154NNK	T154NNK-F		ATTTTAAACCTGGTGATCGCGT
	T154NNK-R		CGTGAAAACC**MNN**AGTCATCATATCGGGAA
C283NNK	C283NNK-F		GTCTTGAATGGGGT**NNK**GGCATGGCTCATA
	C283NNK-R		GTGACGAGCTTAGAAGGATCGA
M285NNK	M285NNK-F		TGGGGTTGCGGC**NNK**GCTCATAAAACTATA
	M285NNK-R		GTGACGAGCTTAGAAGGATCGA
LibA	85+86-F	85AG+86AE-F	GTTGTTGTGCCA**GSAGMA**ACCCCTGATTGGCG
		85AG+86I-F	GTTGTTGTGCCA**GSAATT**ACCCCTGATTGGCG
		85AG+86C-F	GTTGTTGTGCCA**GSATGC**ACCCCTGATTGGCG
	110-F	110IL-F	TGGAATGCTGGCAGGC**MTA**AAATTTTCGAATG
		110E-F	TGGAATGCTGGCAGGC**GAA**AAATTTTCGAATG
		110W-F	TGGAATGCTGGCAGGC**TGG**AAATTTTCGAATG
	110-R	110IL-R	CATTCGAAAATTT**TAK**GCCTGCCAGCATTCCA
		110E-R	CATTCGAAAATTT**TTC**GCCTGCCAGCATTCCA
		110W-R	CATTCGAAAATTT**CCA**GCCTGCCAGCATTCCA
	283+285-F	283C+285MLV-F	GTCTTGAATGGGGT**TGC**GGC**DTG**GCTCATAAAACTAT
		283V+285MLV-F	GTCTTGAATGGGGT**GTG**GGC**DTG**GCTCATAAAACTAT
	283+285-R	283C+285MLV-R	ATAGTTTTATGAGC**CAH**GCC**GCA**ACCCCATTCAAGAC
		283V+285MLV-R	ATAGTTTTATGAGC**CAH**GCC**CAC**ACCCCATTCAAGAC
	294-R	294LV-R	CCACCGGGGCA**TAM**CCCGCCTTTTA
		294T-R	CCACCGGGGCA**GGT**CCCGCCTTTTA

Table S11. Conditions for GC analyses.

Entry	Alcohol	Procedure	Retention time	Reference
1a-b	(*S*)-**1a-b**, (*R*)-**1a-b**	110°C, 5°C /min, 125°C (1 min), 50°C/min, 200°C (1 min). H_2: 1bar Column: Ivadex 25 m x 0.25 mm ID, 0.15 µm.	**1a**: 2.04 min, (*S*)-**2a**: 3.23 min (*R*)-**2a**: 3.07 min **1b**: 2.94 min (*S*)-**2b**: 4.32 min (*R*)-**2b**: 4.23 min	19
1c	(*S*)-**2c**, (*R*)-**2c**	130°C, 3 min, 5°C/min, 138°C, 50°C/min, 200°C. H_2: 1.0 bar Column: Ivadex 25 m x 0.25 mm ID, 0.15 µm.	**1c**: 2.83 min (*S*)-**2c**: 3.9 min (*R*)-**2c**:4.0 min	19
1d	(*S*)-**2d**, (*R*)-**2d**	130°C, 5°C /min, 150°C, 50°C/min, 200°C (1 min). H_2: 1bar Column: Ivadex 25 m x 0.25 mm ID, 0.15 µm.	**1d**: 2.3 min (*S*)-**2d**: 2.9 min (*R*)-**2d**: 3.0 min	19

Table S12. Volume calculated (in Å^3) for WT and A85G/I86A variant in the *apo* state along 100 frames from the MD simulations where the co-factor is not displaced from the enzyme active site. Calculations were done using POVME 2.0.[20]

Enzyme	**Temperature (°C)**	**Average volume (Å^3)**
Wild-type	30	102 ±25
	30	111 ±46
	45	90 ±36
	45	81 ±28
A85G/I86A variant	30	130 ±39
	30	127 ±36
	30	112 ±31
	30	146 ±34
	45	93 ±35
	45	127 ±36
	45	80 ±36

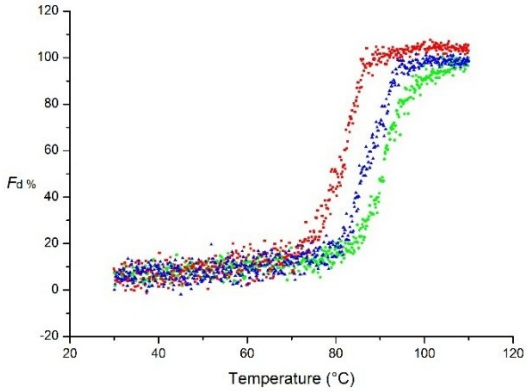

Figure S1. Structural resistance of WT TbSADH(green), TbSADH-1(red) and TbSADH-2(blue) to elevated temperatures was determined as thermal denaturation in phosphate buffer (50 mM, pH 7.4). F_d refers to the unfolded fraction.

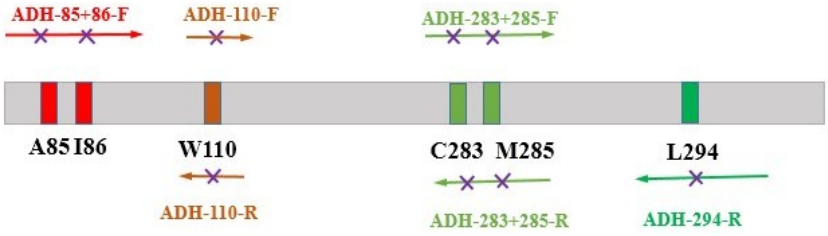

Figure S2. Construction of library A covering positions 85, 86, 110, 283, 285 and 294 using overlap PCR method.

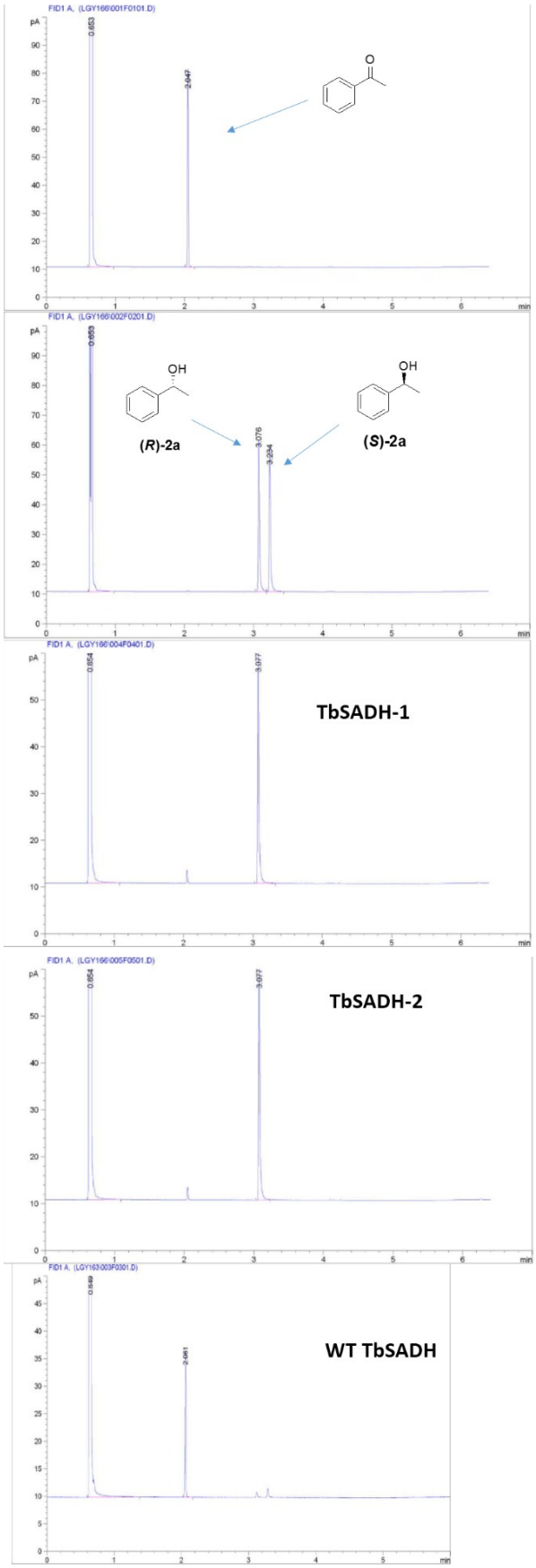

Figure S3. GC profiles of **1a** to **2a**

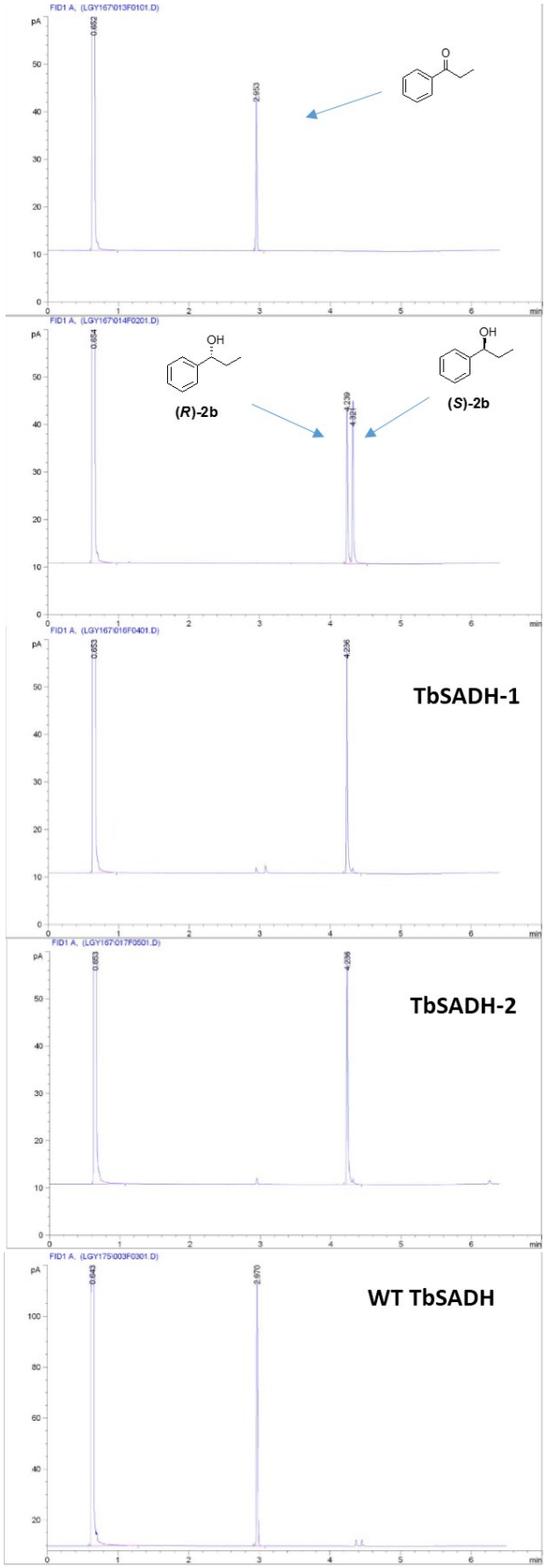

Figure S4. GC profiles of **1b** to **2b**

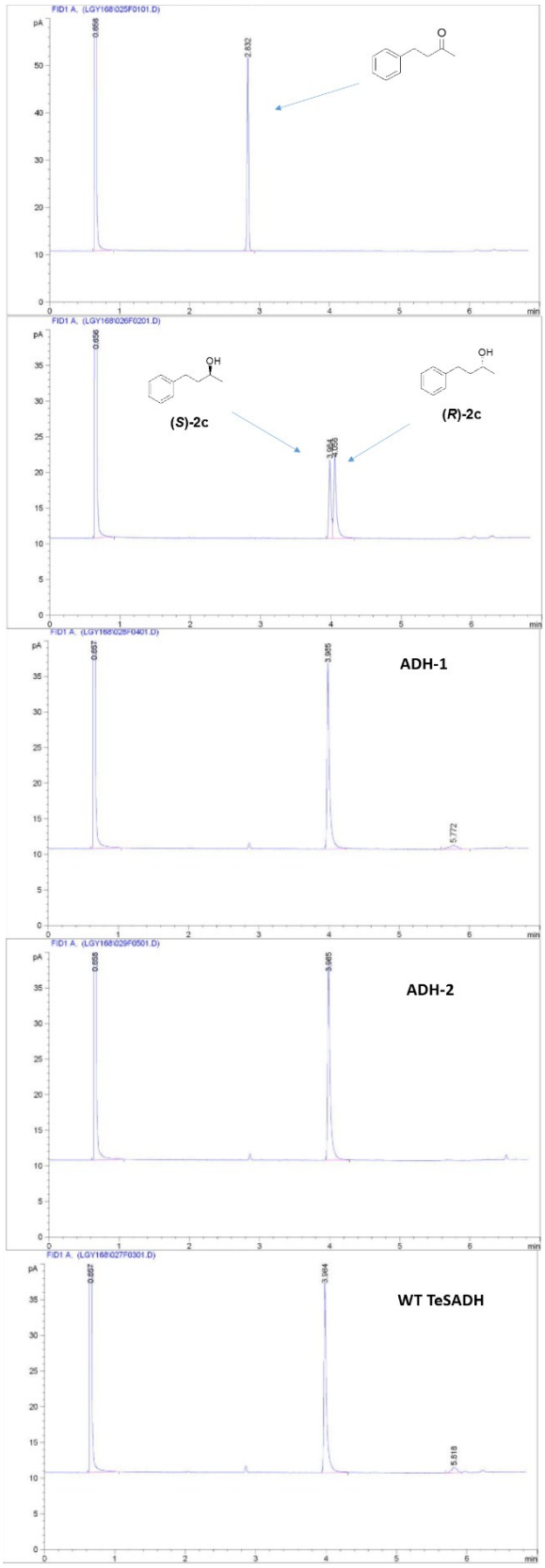

Figure S5. GC profiles of **1c** to **2c**

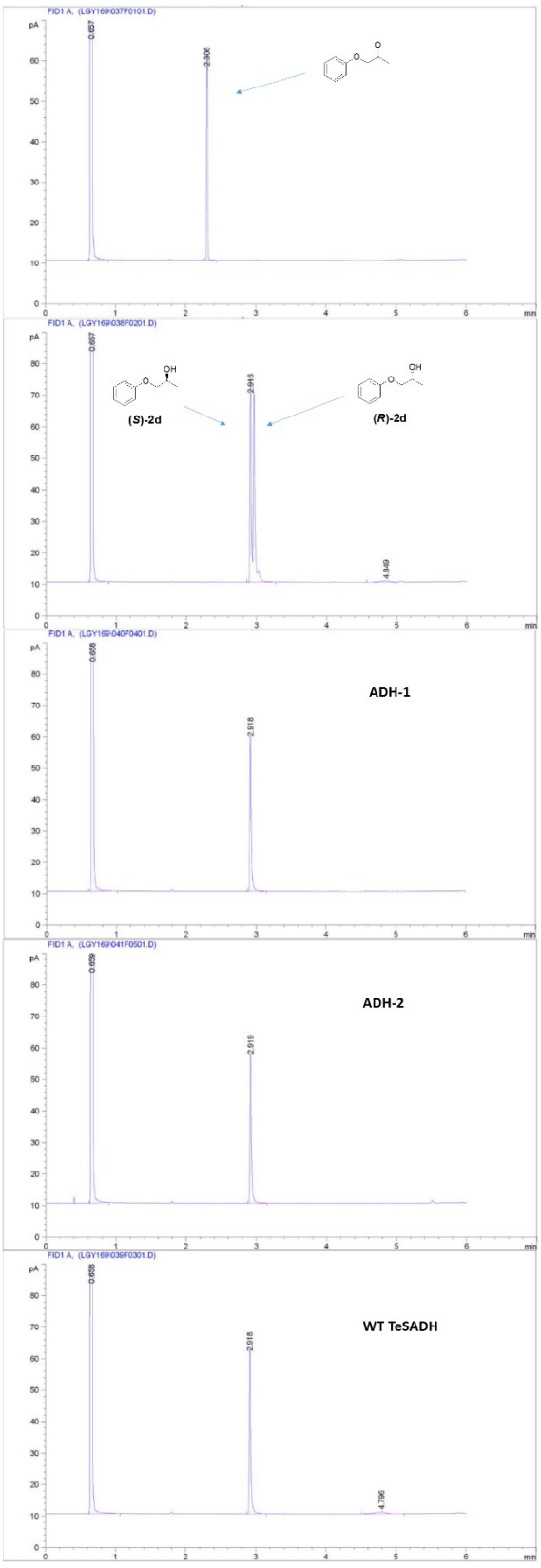

Figure S6. GC profiles of **1d** to **2d**

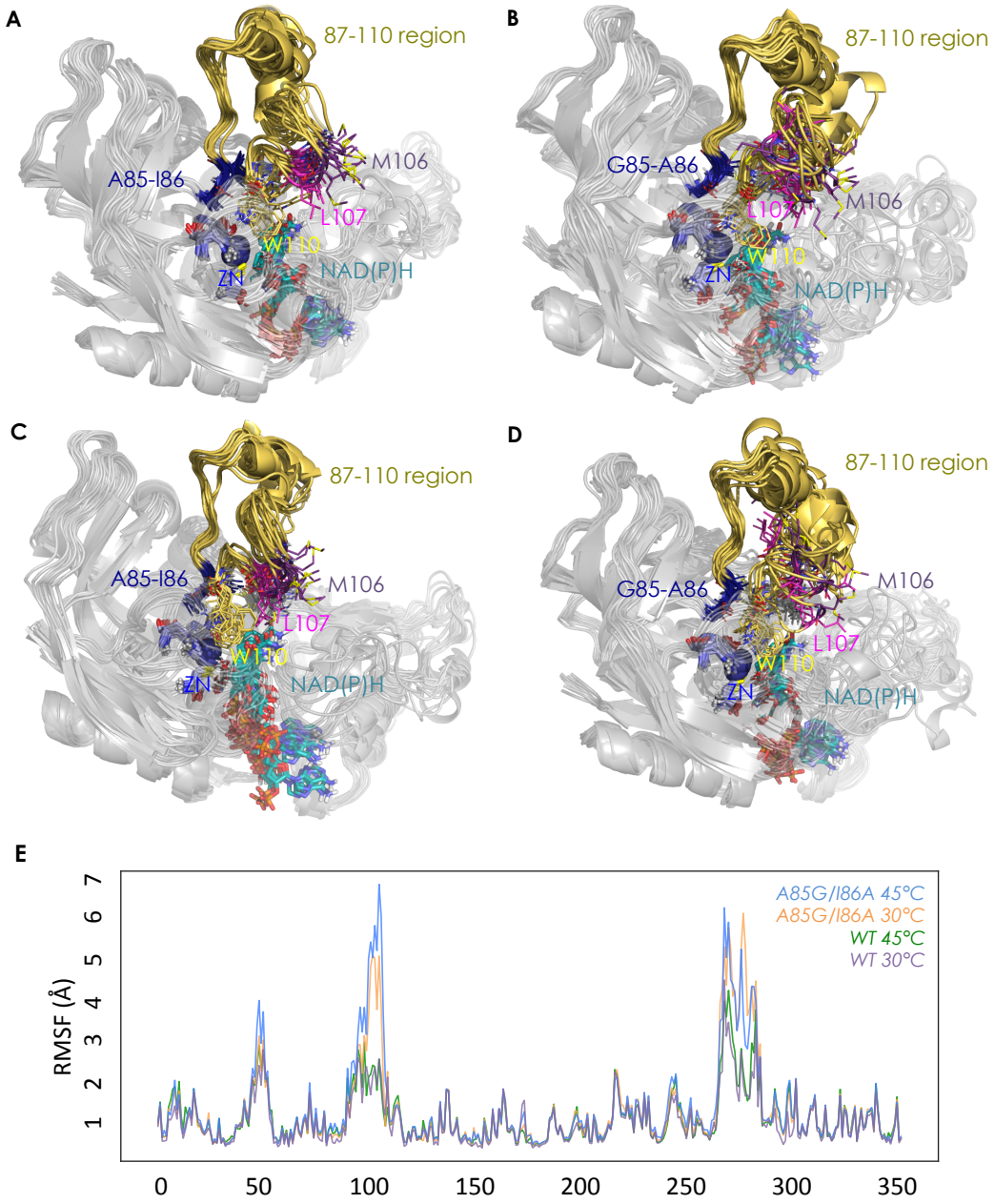

Figure S7. Overlay of some representative MD snapshots for WT (**A** 30°C**, C** 45°C) and A85G/I86A variant (**B** 30°C, **D** 45°C) in the *apo* state. Average values of Root Mean Square Fluctuation (RMSF) of all residues computed from the MD simulations (where the cofactor is not displaced from the active site) in *apo* state (**E**)

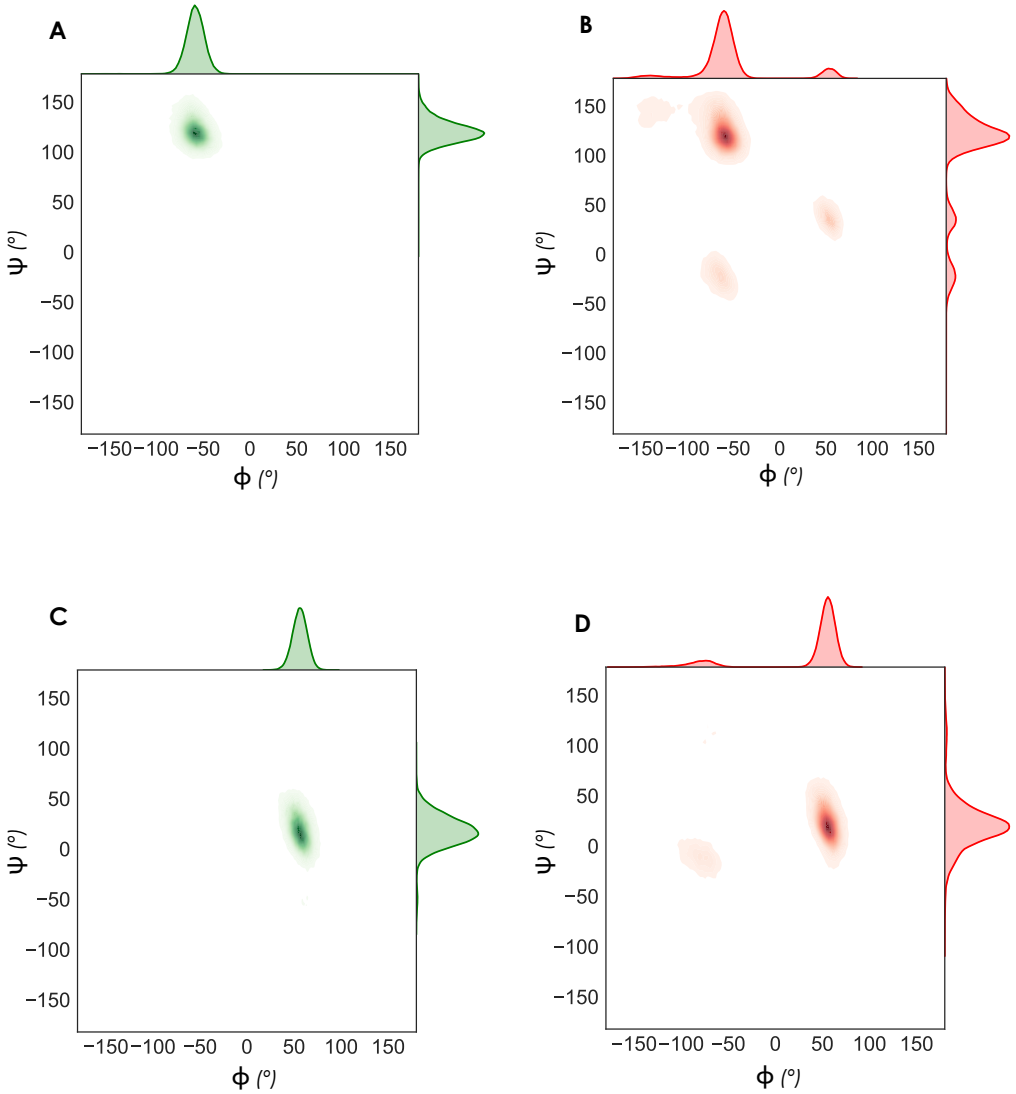

Figure S8. Representation of the Ramachandran plots esidues M106 (**A**, **B**), and L107 (**C**, **D**) for WT en) and A85G/I86A variant (red) for all MD ulations in the *apo* state at 30°C.

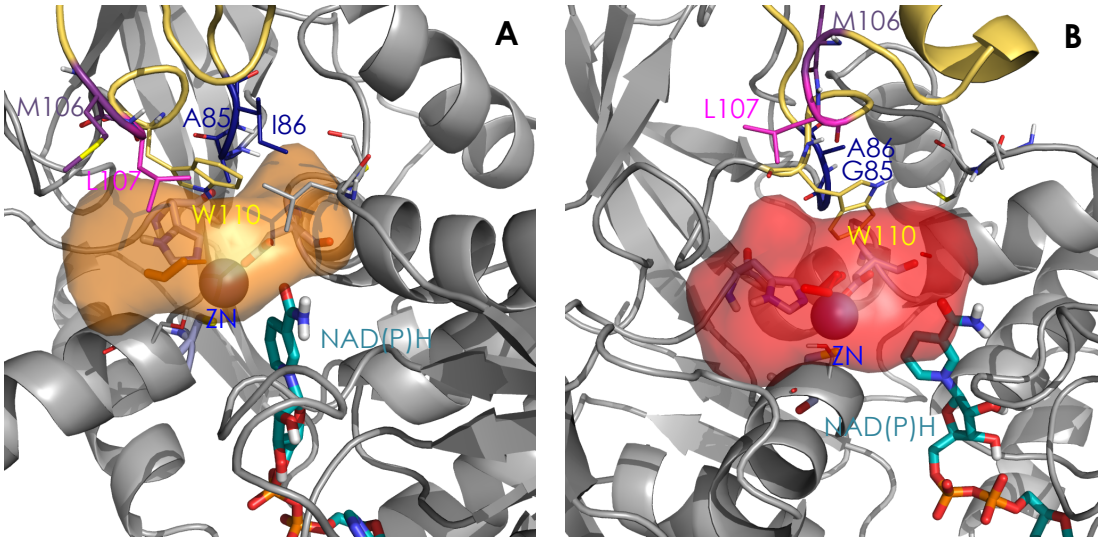

Figure S9. Active site volume representation of the most populated cluster from the MD simulations in the state for WT (**A**), and A85G/I86A variant (**B**). These calculations have been performed with POVME[20]

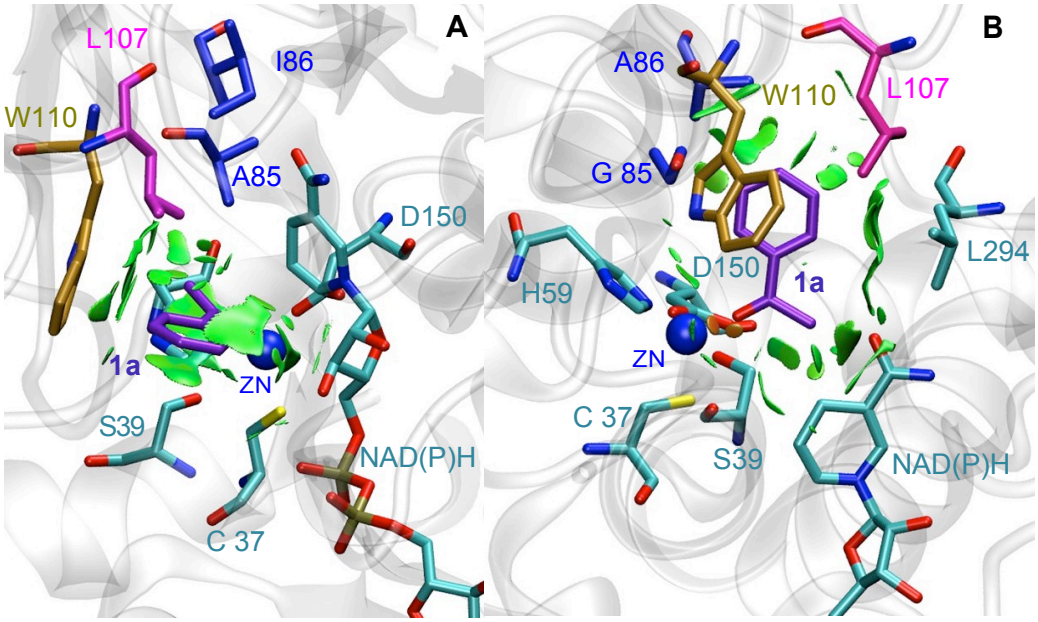

Figure S10. Representations of the most important non-covalent interactions (in green) between the substrate **1a** and the active site for WT (**A**) and A85G/I86A variant (**B**), computed with the computational tool NCIplot.[21]

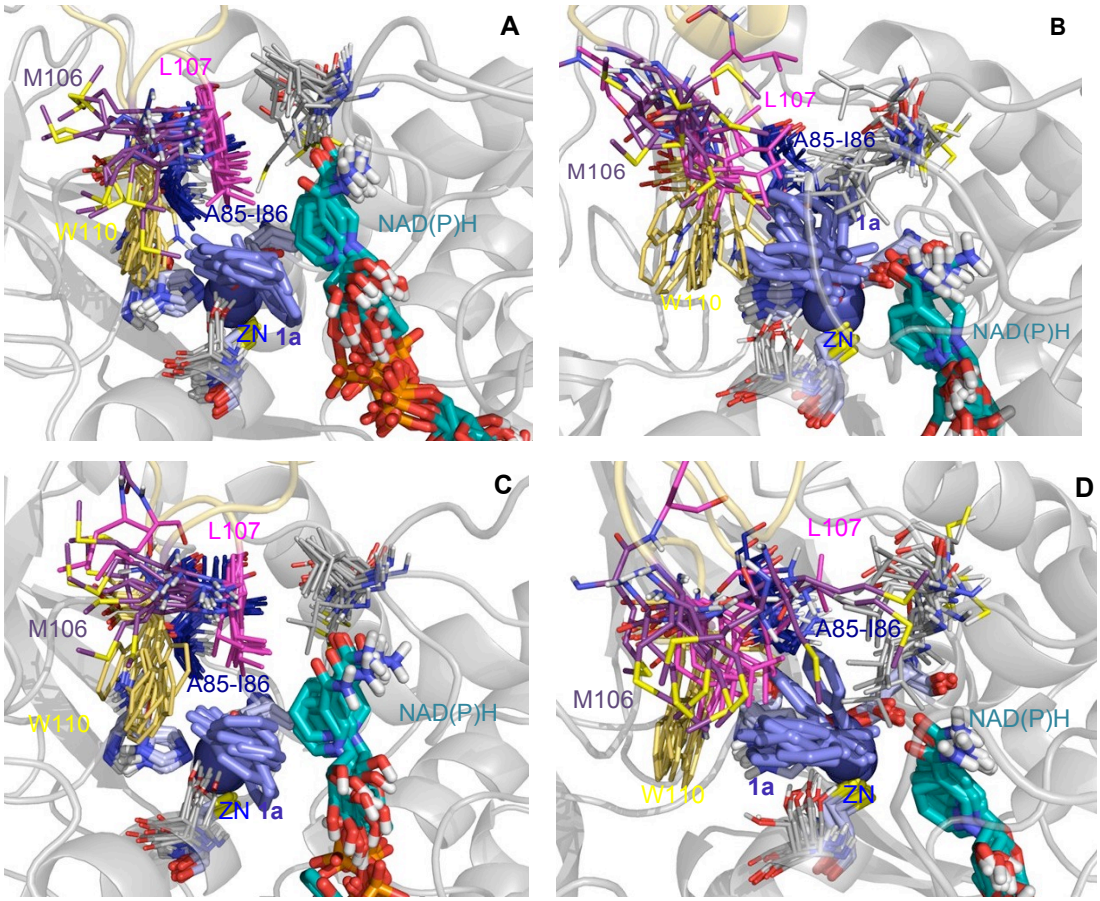

Figure S11. Overlay of some representative MD snapshots for WT with **1a** in *pro*-(S) conformation (**A** 30°C, **C** 45°C) and A85G/I86A variant with 1a in *pro*-(R) conformation (**B** 30°C , **D** 45°C).

References

1. Korkhin, Y.; Kalb, A. J.; Peretz, M.; Bogin, O.; Burstein, Y.; Frolow, F. *J. Mol. Biol,* **1998**, *278*, 967.
2. Sun, Z.; Lonsdale, R.; Ilie, A.; Li, G.; Zhou, J.; Reetz, M. T. *ACS. Catal,* **2016**, *6*, 1598.
3. Bougioukou, D. J.; Kille, S.; Taglieber, A.; Reetz, M. T. *Adv. Synth. Catal,* **2009,** *351*, 3287-3305.
4. Case, D. A.; Darden, T. A.; Cheatham, T. E.; Simmerling, C. L.; Wang, J.; Duke, R. E.; et al. AMBER 16, University of California, San Francisco, 2016.
5. Wang, J.; Wolf, R. M.; Caldwell, J. W.; Kollman, P. A.; Case, D. A. *J. Comput. Chem*, **2004**, *25*, 1157-1174.
6. Bayly, C. I.; Cieplak, P.; Cornell, W.; Kollman, P. A. *J. Phys. Chem*, **1993**, *97*, 10269-10280.
7. Bessler, B.; Merz Jr, K.; Kollman, P. *J. Comput. Chem*, **1990**, *11*, 431-439.
8. Singh, U. C.; Kollman, P. A. *J. Comput. Chem*, **1984**, *5*, 129-145.
9. M. J. Frisch GWT, H. B. Schlegel, G. E. Scuseria, M. A. Robb, J. R. Cheeseman, G. Scalmani, V. Barone, G. A. Petersson, H. Nakatsuji, X. Li, M. Caricato, A. Marenich, J. Bloino, B. G. Janesko, R. Gomperts, B. Mennucci, H. P. Hratchian, J. V. Ortiz, A. F. Izmaylov, J. L. Sonnenberg, D. Williams-Young, F. Ding, F. Lipparini, F. Egidi, J. Goings, B. Peng, A. Petrone, T. Henderson, D. Ranasinghe, V. G. Zakrzewski, J. Gao, N. Rega, G. Zheng, W. Liang, M. Hada, M. Ehara, K. Toyota, R. Fukuda, J. Hasegawa, M. Ishida, T. Nakajima, Y. Honda, O. Kitao, H. Nakai, T. Vreven, K. Throssell, J. A. Montgomery, Jr., J. E. Peralta, F. Ogliaro, M. Bearpark, J. J. Heyd, E. Brothers, K. N. Kudin, V. N. Staroverov, T. Keith, R. Kobayashi, J. Normand, K. Raghavachari, A. Rendell, J. C. Burant, S. S. Iyengar, J. Tomasi, M. Cossi, J. M. Millam, M. Klene, C. Adamo, R. Cammi, J. W. Ochterski, R. L. Martin, K. Morokuma, O. Farkas, J. B. Foresman, and D. J. Fox. Gaussian 09, Revision A. 02. Gaussian. Inc: Wallingford, CT 2009.
10. Anandakrishnan, R.; Aguilar, B.; Onufriev, A. V. *Nucleic. Acids. Res,* **2012,** *40*, W537-W541.
11. G. V. Dhoke, M. D. Davari, U. Schwaneberg, M. Bocola. *ACS Catal,* **2015**, *5*, 3207-3215.
12. Seminario, J.M. *Int. J. Quantum. Chem*, **1996**, *60*, 1271-1277.
13. Hu, L.; Ryde, U. J. *Chem. Theory. Comp*, **2011**, *7*, 2452-2463.
14. Ryde, U. *Protein Sci*, **1995**, *4*, 1124-1132.
15. Ryde, U. *J. Chem. Phys*, **1983,** *79*, 926-935.
16. Jorgensen, W. L.; Chandrasekhar, J.; Madura, J. D.; Impey, R. W.; Klein, M. L. *J. chem. phys,* **1983**, *79*, 926-935.
17. Hornak, V.; Abel, R.; Okur, A.; Strockbine, B.; Roitberg, A.; Simmerling, C. *Proteins: Structure, Function, and Bioinformatics*, **2006**, *65*, 712-725.
18. Darden, T.; York, D.; Pedersen, L. *J. Chem. Phys,* **1993**, *98*, 10089-10092.
19. Sun, Z.; Li, G.; Ilie, A.; Reetz, M. T. *Tetrahedron. Lett,* **2016**, *57*, 3648.
20. J. D. Durrant, L. Votapka, J. Sørensen, R. E. Amaro, J. *Chem. Theory. Comp,* **2014**, *10*, 5047-5056.
21. a) J. Contreras-García, E. R. Johnson, S. Keinan, R. Chaudret, J.-P. Piquemal, D. N. Beratan, W. Yang, J. *Chem. Theory. Comp,* **2011**, *7,* 625-632. b) E. R. Johnson, S. Keinan, P. Mori-Sanchez, J. Contreras-Garcia, A. J. Cohen, W. Yang, *J. Am. Chem. Soc,* **2010**, *132*, 6498-6506.